Supplementary Materials

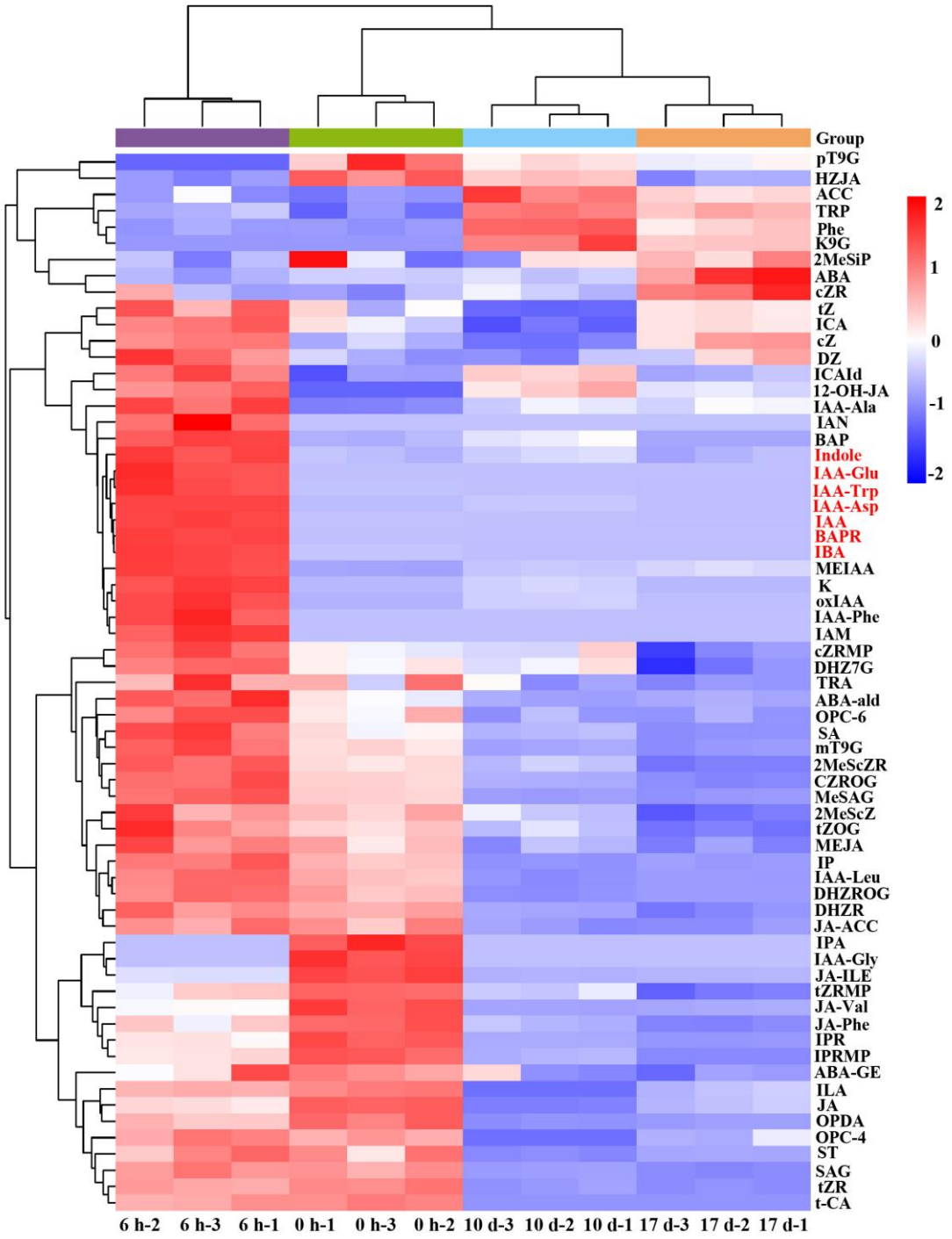


Figure S1. Heatmap analysis of phytohormone contents in the phloem at the base of cuttings at 0 h (wounding) and 6 h, 10 d and 17 d after planting. The full names, classifications and contents of the corresponding hormones are listed in Table S1.

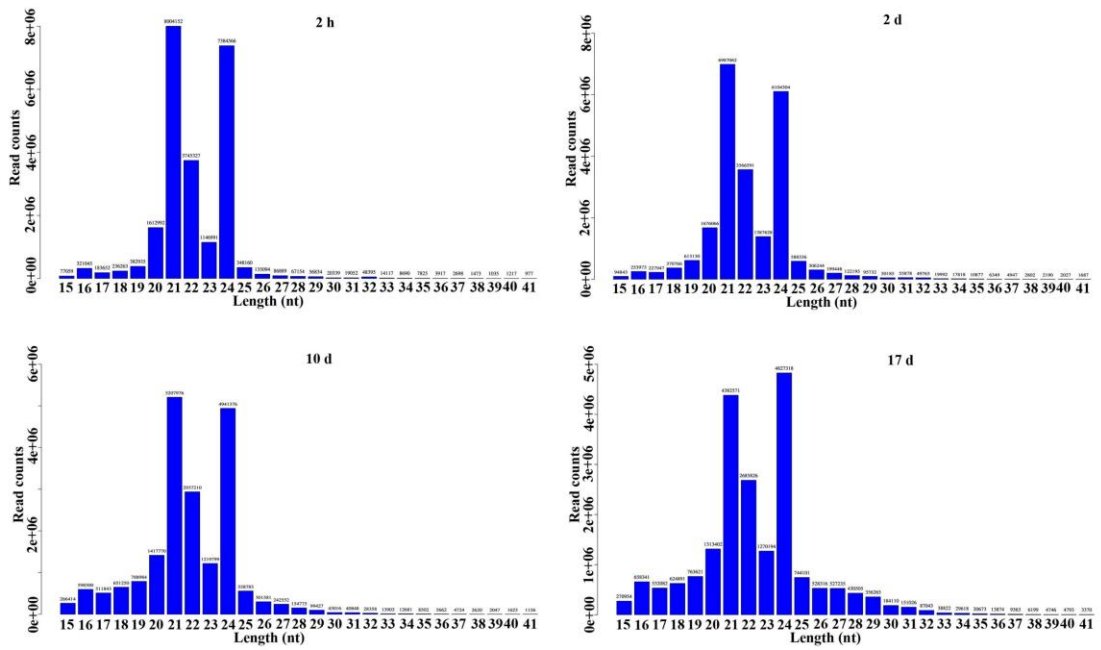


Figure S2. The length distribution of clean reads. The number on top of each bar indicates the number of clean read of that length.

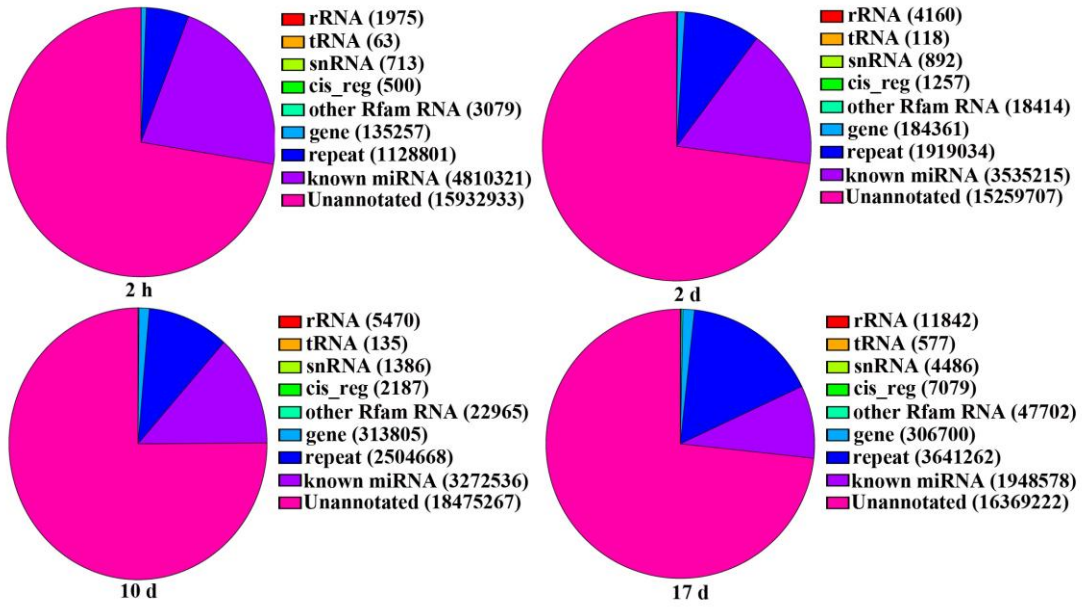


Figure S3. Pie chart illustrating the classification of reads detected in 2 h, 2 d, 10 d, and 17 d samples. The numbers of reads for each category is shown in parentheses.

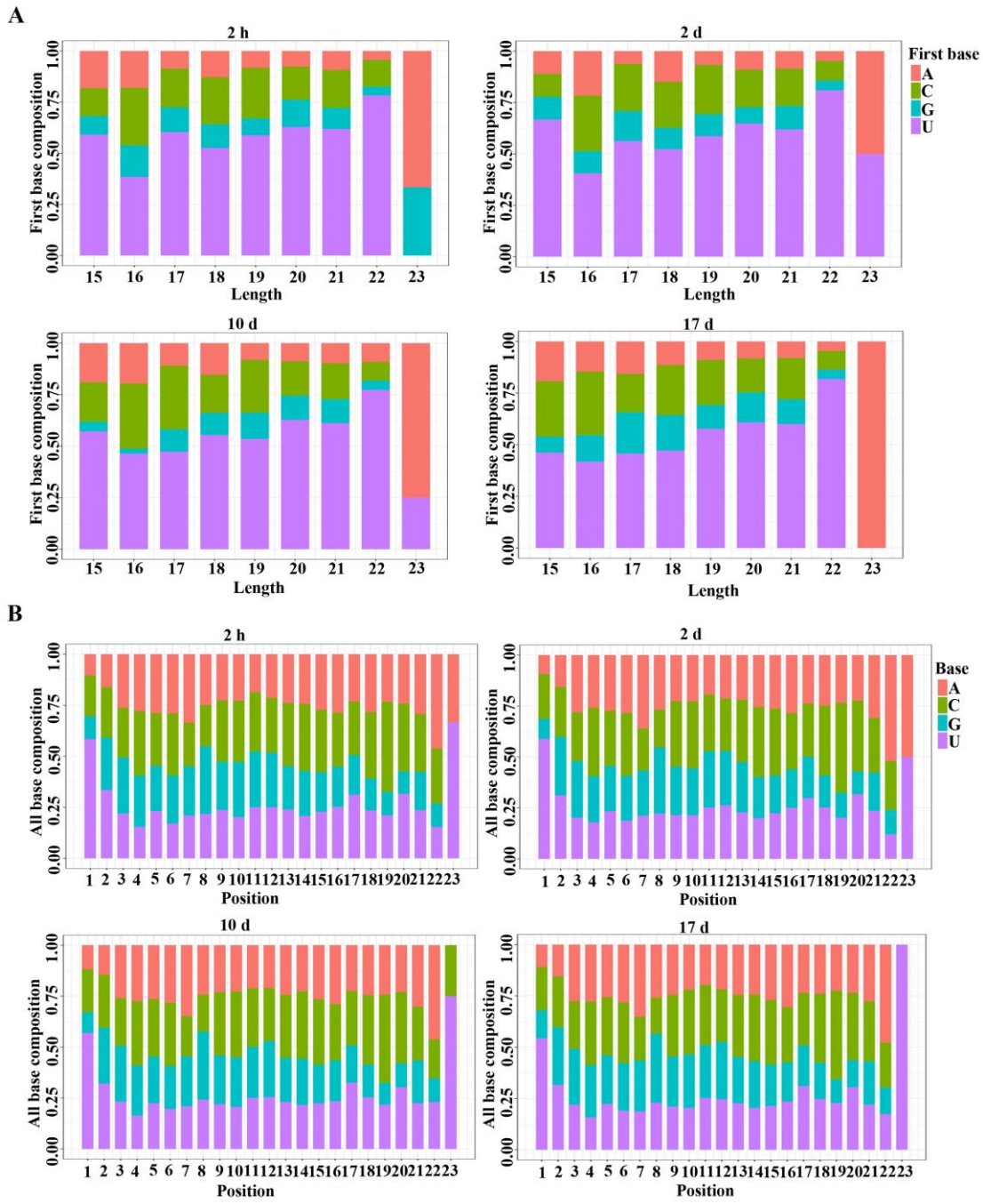


Figure S4. Nucleotide preference analysis of known miRNA. (A) Nucleotide distribution at the first position of miRNA. (B) Nucleotide distribution at each position.

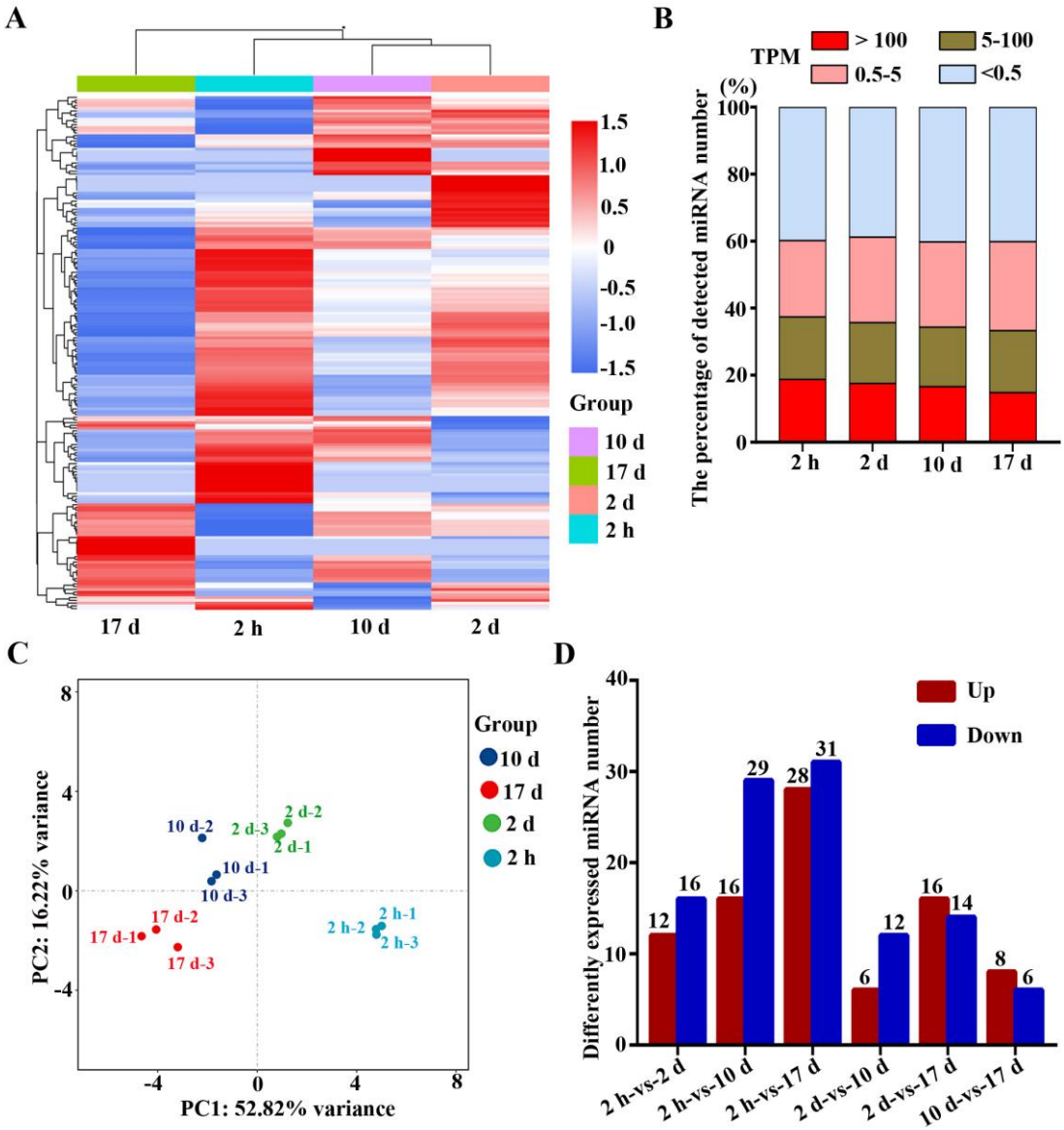


Figure S5. Preliminary miRNAomic analysis of peach rootstock cuttings at four time points during the rooting process. (A) Heatmap showing the fold changes of miRNAs in the comparison group libraries. (B) Proportion of miRNAs in different expression abundance ranges. (C) Principal Component Analysis (PCA) of miRNA expression data. (D) Total number of up-regulated and down-regulated differentially expressed (DE) miRNAs in the four comparison groups.

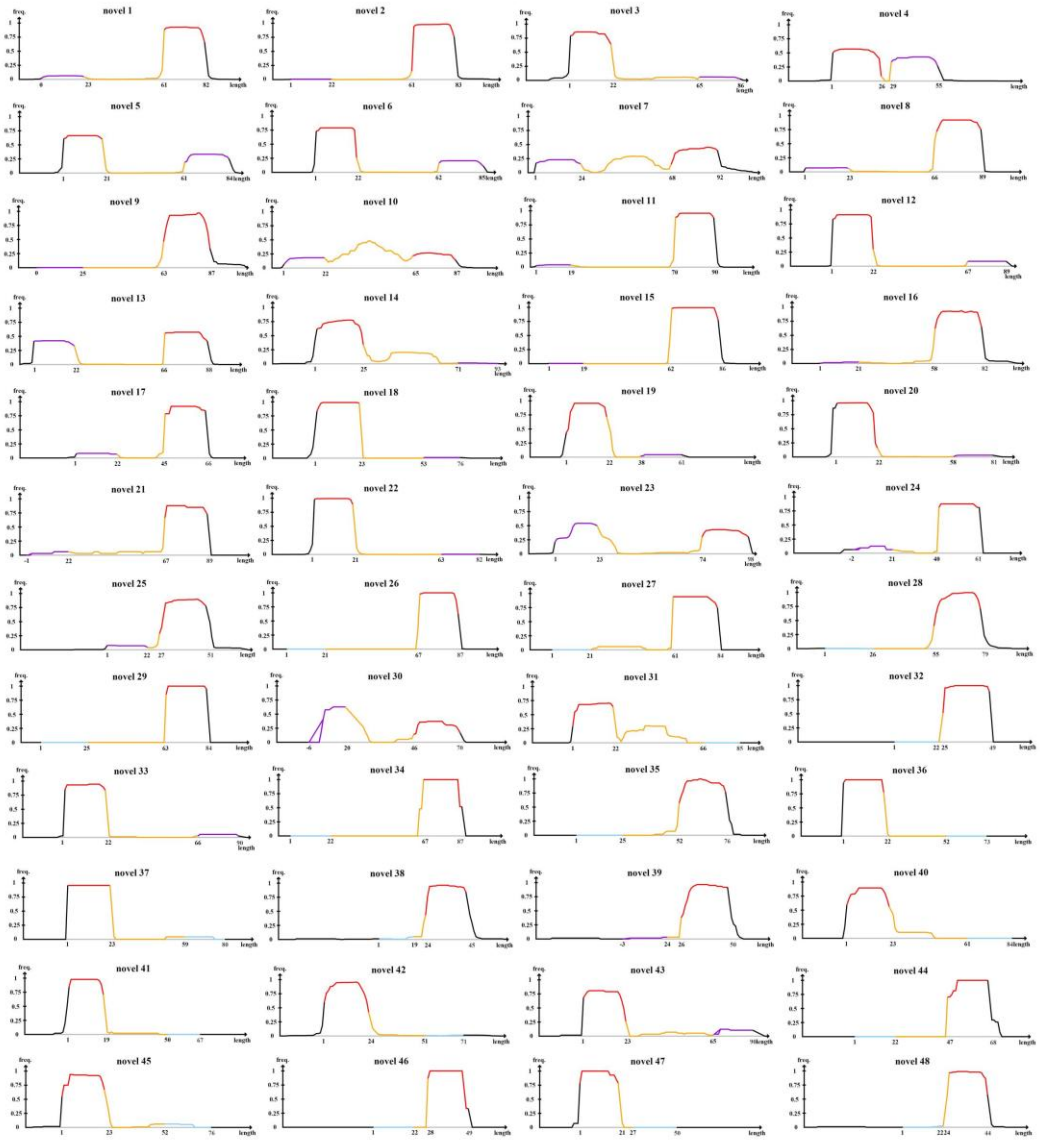


Figure S6. Novel miRNA structure diagram. The X-axis represents the length of the precursor sequence, and the Y-axis indicates the frequence of sequencing reads. The one or two prominent peaks at specific locations (highlighted in purple and red) correspond to the two arms of the hairpin stem. The yellow region denotes the loop of the hairpin structure. Each peak represents a mature miRNA: the peak on the 5' arm corresponds to miR-5p, while the peak on the 3' arm corresponds to miR-3p.

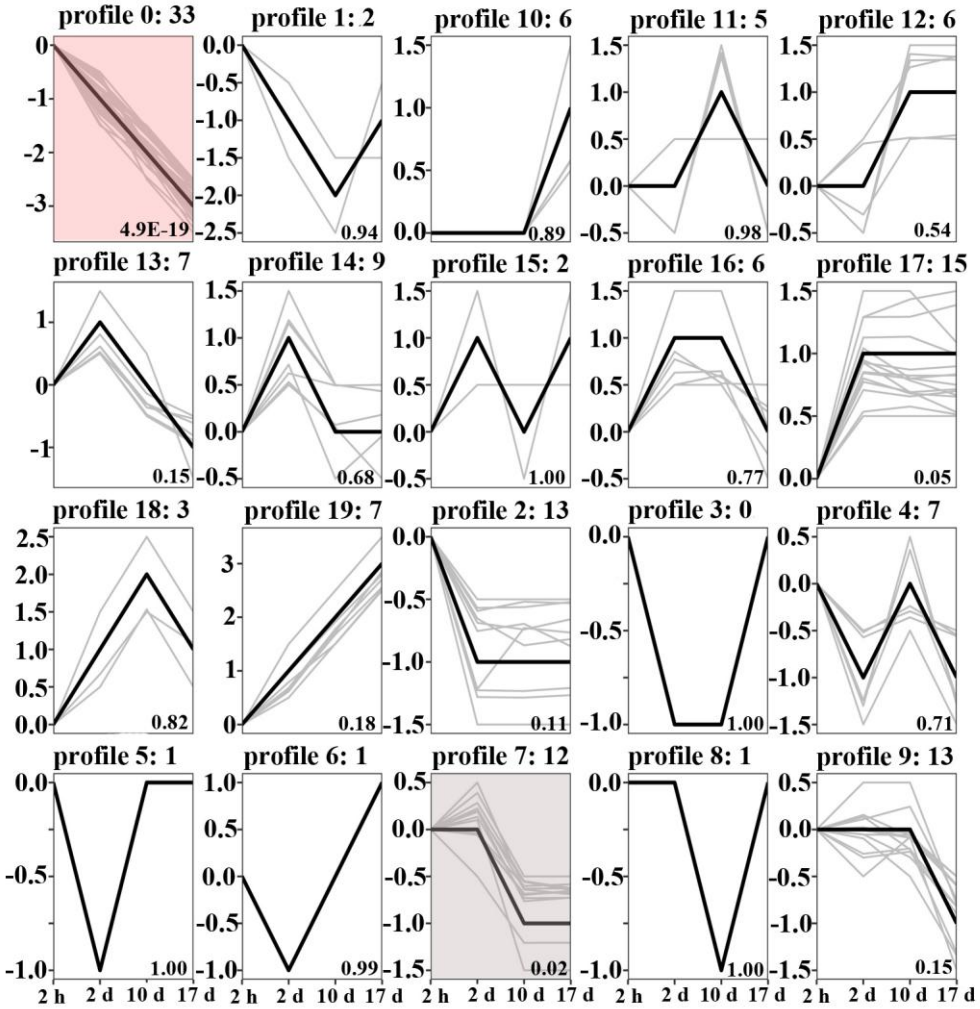


Figure S7. Trend clustering of detected miRNAs during AR formation. For each expression profile, the number following the colon represents the miRNA number belonging to that profile, while the corresponding *p*-value is displayed in the lower right corner.

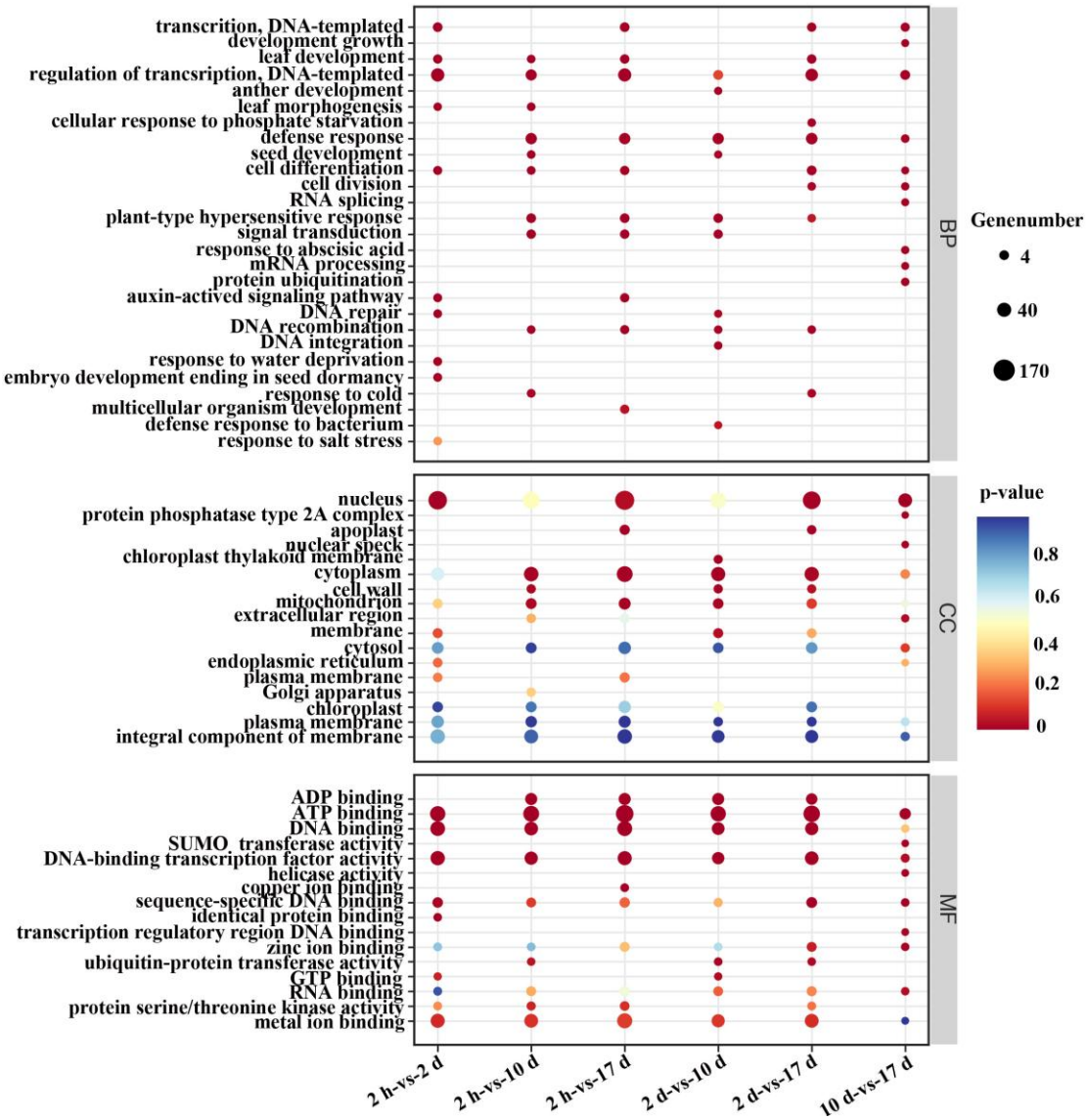


Figure S8. Comprehensive Gene Ontology (GO) enrichment analysis of target genes for differentially expressed miRNAs from the four comparison groups (2 h vs. 2 d, 2 d vs. 10 d, 2 d vs. 17 d, 10 d vs. 17 d). BP: Biological process, CC: Cellular component, MF: Molecular function.

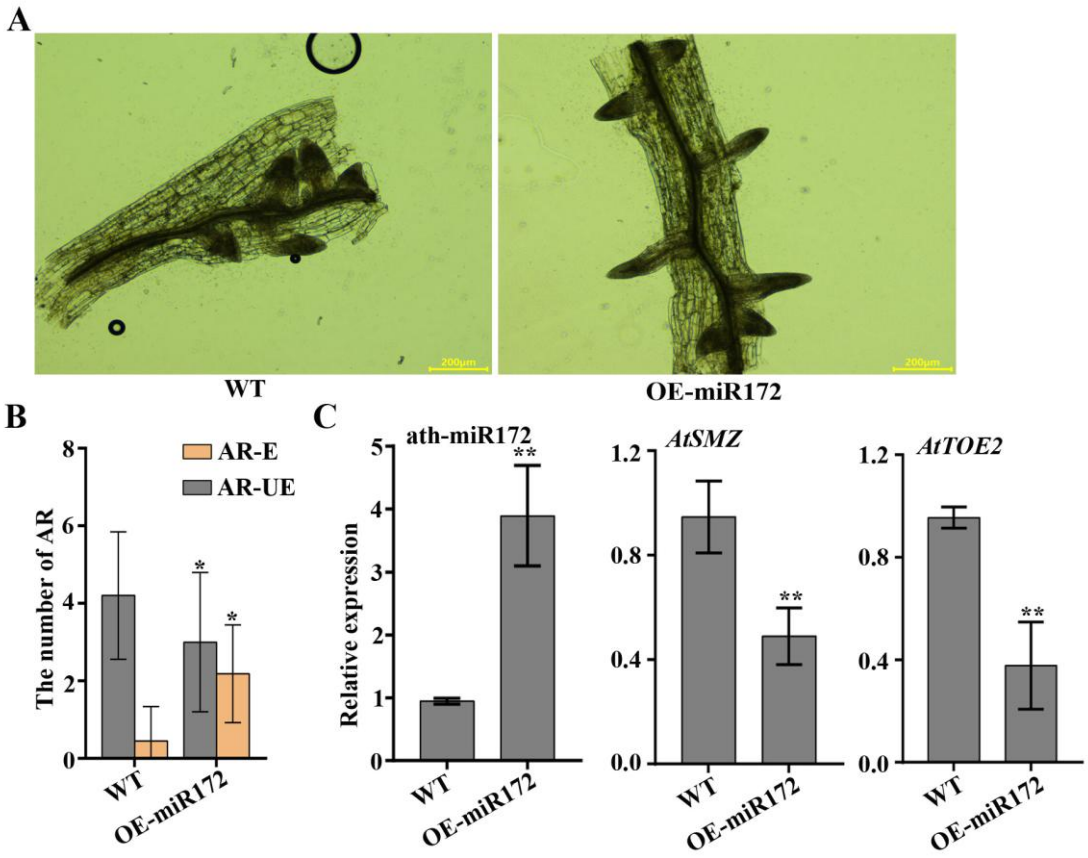


Figure S9. Phenotypic characterization of WT and over expression miR172 Arabidopsis. (A) Images of WT and transgenic Arabidopsis. (B) Number of AR per hypocotyl for different genotypes at 3 days after primary root removal (n=20). AR-E represents emerged adventitious roots that have broken through the epidermis, AR-UE represents unemerged adventitous roots that have not. (C) Relative expression levels of ath-miR172 and its targt genes determined by qRT-PCR. Asterisks indicate significant differences compared to the WT, as determined by a two-tailed Student's t-test (* $p < 0.05$ and ** $p < 0.01$). Error bars represent the standard error between three biological replicates (n=3). The OE-miR172 line 3 was used for this study.

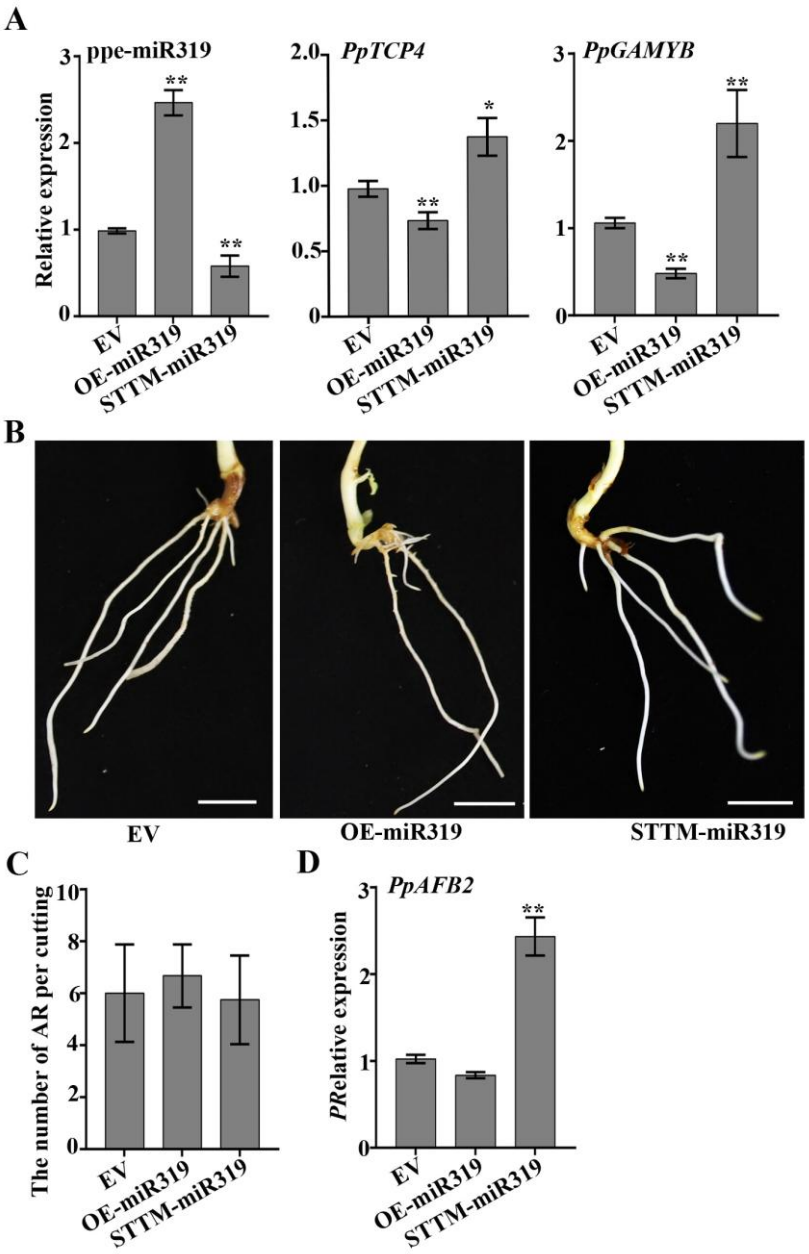


Figure S10. Phenotypic characterization of peach seedlings with different genes transformed. (A) Relative expression levels of ppe-miR319 and its target genes determined by qRT-PCR. (B) Images of transgenic and EV (empty plasmid) peach seedlings. Scale = 1 cm. (C) Number of AR per hypocotyl for different genotypes after primary root removal (n=8 seedlings per genotype). (D) Relative expression levels of *PpAFB2* determined by qRT-PCR. Error bars represent the standard error between three biological replicates (n=3). Asterisks indicate significant differences compared to the WT, as determined by a two-tailed Student's *t*-test (* $p < 0.05$ and ** $p < 0.01$).